

Modelling Band-to-Band Tunneling Current in InP-based Heterostructure Photonic Devices

J.P. van Engelen, L. Shen, J.J.G.M. van der Tol, M.K. Smit

Photonic Integration Research Group, Dept. of Electrical Engineering,
Eindhoven University of Technology, Postbus 513, 5600 MB Eindhoven, The Netherlands

Some semiconductor photonic devices show large discontinuities in the band structure. Short tunnel paths caused by this band structure may lead to an excessive tunnelling current, especially in highly doped layers. Modelling of this tunnelling current is therefore important when designing photonic devices with such band structures. The traditional Kane's tunnelling model can only be applied to homostructures. An extension to heterostructures is developed to study interband tunneling probability in InP-based heterostructures and the resulting tunnelling current is calculated.

Introduction

We are developing a membrane-based photonic device with a highly doped ($N_e = 10^{18} - 10^{19} \text{cm}^{-3}$) junction which will be operated in reverse bias. In highly doped reverse biased pn-junctions significant tunneling current can occur. Because cooling of devices in membranes is still a problem it is important that the device has a low tunneling current and therefore a low power consumption. Most research on Band-To-Band Tunneling (BTBT), such as Kane's model [1], applies only to homojunctions, while InP-based photonic devices often contain heterojunctions with large discontinuities in the band structure at material interfaces. Figure 1 shows the band structure of a highly-doped reverse-biased pin heterojunction. It is clear that the discontinuities in the conduction and valance bands have a large influence on the tunneling probability of electrons across the junction. In this paper we describe how to model the tunneling current in heterojunctions and how to determine the breakdown voltage due to tunneling.

Theory

Band-To-Band tunneling in highly doped p-n junctions can be significant if the tunneling path (at constant electron energy) from valance band to conduction band is sufficiently small. The tunneling path starts at the classical turning point x_v where the electron energy equals the valance band edge energy, the tunneling path stops at the classical turning point x_c where the electron energy equals the conduction band edge energy. This tunneling path is indicated by the dotted line in Figure 2a. The WKB approximation is used to calculate the probability of tunneling P : [2]

$$P = |T|^2 \approx \exp\left(-2 \int_{x_v}^{x_c} |k(x)| dx\right), \quad (1)$$

with T the transmission coefficient and $k(x)$ the wavevector. A triangular barrier is based on the assumption that a tunneling electron suddenly changes its potential energy at x_v [3,

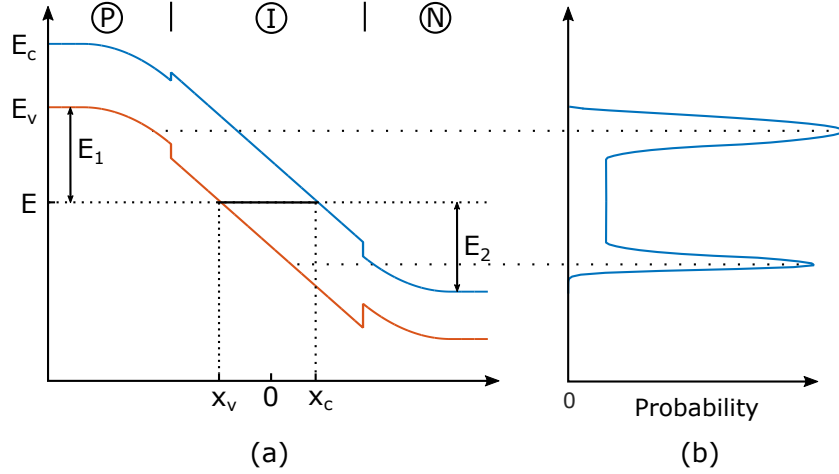


Figure 1: (a) Band diagram of a reverse-biased pin heterojunction with matching tunneling probability (b). The shortest paths show the highest probability.

p. 484]. A more realistic barrier follows from the one-dimensional two-band Schrödinger equation and yields a parabolic barrier [4]:

$$k(x) = \frac{1}{\hbar} \sqrt{\frac{2m_r}{E_g} (E_c(x) - E)(E - E_v(x))}, \quad (2)$$

with m_r the reduced mass as defined in [3, p. 484] and E the energy of the electron. Assuming a constant electric field \mathcal{E} , $|k(x)|$ can be rewritten as [3, 4]:

$$k(x) = \frac{1}{\hbar} \sqrt{\frac{2m_r}{E_g} \left(\left(\frac{E_g}{2} \right)^2 - (q\mathcal{E}x)^2 \right)}, \quad (3)$$

and centering x_v and x_c around 0 we have [3]:

$$T \approx \exp \left(-2 \int_{-l/2}^{l/2} |k(x)| dx \right) = \exp \left(-\frac{\pi \sqrt{2m_r} E_g^{3/2}}{4 q \hbar \mathcal{E}} \right), \quad (4)$$

where $l = E_g/(q\mathcal{E})$. Tunnel paths through a heterogeneous junction experience a discontinuity of $k(x)$ at the interface because E_g , m_r , the permittivity ε and the electron affinity χ_e are different in each material. The discontinuity is shown in Figure 2b. We split the integral in two parts:

$$\int_{-x_v}^{x_c} |k(x)| dx = \int_{-l_1/2}^{-l_1/2+x_v} |k_1(x)| dx + \int_{l_2/2-x_c}^{l_2/2} |k_2(x)| dx = I_1(x_v) + I_2(x_c); \quad (5)$$

As the two integrals are similar (the integrals equal the surface of a section of a semi-circle, Figure 2b):

$$I_i(x) = \frac{q\mathcal{E}}{\hbar} \sqrt{\frac{2m_{r,i}}{E_{g,i}}} \int_{-l_i/2}^{-l_i/2+x} \sqrt{\left(\frac{l_i}{2} \right)^2 - x'^2} dx'; \quad (6)$$

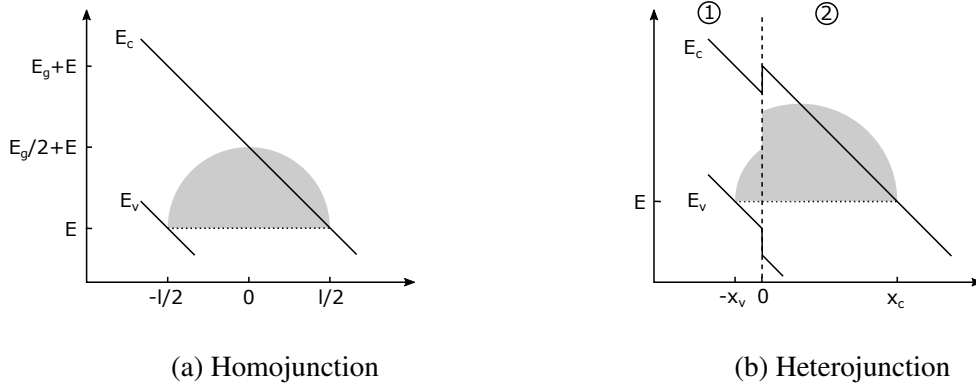


Figure 2: Energy band diagram of two semiconductor junctions. The tunneling path is indicated by the dotted line and the shaded area represents the integral over the wavevector for the electron with energy E .

we can write down a general solution $I_i(x)$ for both:

$$I_i(x) = \frac{q\mathcal{E}}{2\hbar} \sqrt{\frac{2m_{r,i}}{E_{g,i}}} \left(x - \frac{l_i}{2}\right) \sqrt{\left(\frac{l_i}{2}\right)^2 - \left(x - \frac{l_i}{2}\right)^2} + \frac{q\mathcal{E}}{2\hbar} \sqrt{\frac{2m_{r,i}}{E_{g,i}}} \left(\frac{l_i}{2}\right)^2 \arcsin\left(1 - \frac{2x}{l_i}\right). \quad (7)$$

Using this solution, the tunneling probability through the heterojunction is:

$$P \approx \exp(-2I_1(x_v) - 2I_2(x_c)) \quad (8)$$

Effect of Transverse Energy

The model in (2) assumes that all the energy of the electron can be used for tunneling. In reality the transverse energy E_{\perp} cannot be used for tunneling [4]. Solving the two-band Schrödinger equation to include E_{\perp} yields the substitution: $E_c \mapsto E_c + E_{\perp}$, $E_v \mapsto E_v - E_{\perp}$ and $E_g \mapsto E_g + 2E_{\perp}$ in $k(x)$:

$$k(x) = \frac{1}{\hbar} \sqrt{\frac{2m_r}{E_g + 2E_{\perp}} (E_c(x) + E_{\perp} - E)(E - E_v(x) + E_{\perp})}. \quad (9)$$

The tunneling probability now depends both on the total energy E and the transverse component of the energy E_{\perp} of the electron. E_{\perp} varies between 0 and E_s , where E_s is the smaller of E_1 and E_2 (as defined in Figure 1) [1]. Note that the introduction of the transverse energy does not change the classical turning points x_v and x_c . For completeness, the tunnel current is given by [4, 5]:

$$J_t = \frac{qm_r}{2\pi^2\hbar^3} \int_{E_{c_n}}^{E_{v_p}} (F_C(E) - F_V(E)) \int_0^{E_s} T(E, E_{\perp}) dE_{\perp} dE, \quad (10)$$

where E_{c_n} is the edge energy of the conduction band at the n-side of the junction and E_{v_p} the valance band at the p-side.

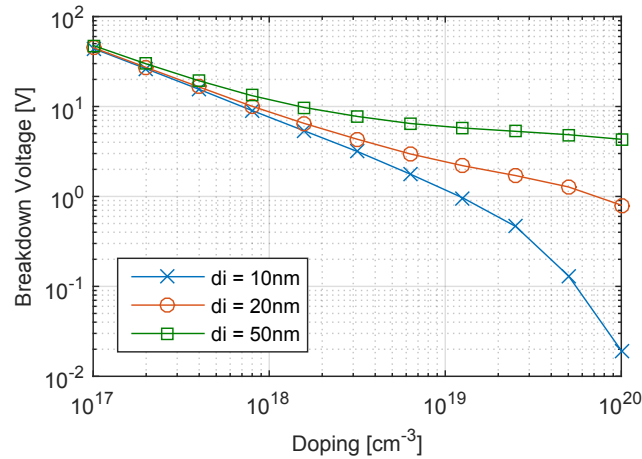


Figure 3: Breakdown voltage as a function of doping. Higher doping and narrower intrinsic region d_i have a lower breakdown voltage.

Numerical Study

In the previous sections we assumed a constant electric field in (3). In practice this is only the case in intrinsic semiconductor layers. If the electric field is constant, $T(E, E_{\perp})$ has an analytic solution, but in other cases we need to calculate the tunneling probability and total tunneling current numerically from (9) and (10). We can now define the breakdown voltage due to tunneling as the voltage at which the tunnel current exceeds a threshold. From experience we set the breakdown current at 3mA; higher current is found to cause thermal damage to our membrane devices. Results are shown in Figure 3 for a pin junction with doped Q1.25 regions and intrinsic InP region. High electric fields cause high tunneling probability, the result is a decrease of the breakdown voltage with increasing doping and narrower intrinsic region.

Summary

We present a theoretical model of tunneling probability across hetero junctions and the resulting tunneling current. The results were used to determine the breakdown voltage due to tunneling for a InP-based hetero pin junction. This model can be used for membrane photonic devices where high electric fields are used and where heating effects should be minimized.

References

- [1] E.O. Kane. Theory of tunneling. *Journal of Applied Physics*, 32(1):83–91, 1961.
- [2] D.J. Griffiths. *Introduction to Quantum Mechanics*. Pearson Education India, 2005.
- [3] S Wang. *Fundamentals of Semiconductor Theory and Device Physics*. Prentice-Hall International Editions, 1989.
- [4] R.Q. Yang, M. Sweeny, D. Day, and J.M. Xu. Interband tunneling in heterostructure tunnel diodes. *Electron Devices, IEEE Transactions on*, 38(3):442–446, Mar 1991.
- [5] *Atlas User's Manual*. Silvaco Inc., 2013.